Multiple changes in rate-determining step in the acid and base catalyzed cyclizations of ethyl *N*-(*p*-nitrophenyl)hydantoates caused by methyl substitution

Iva B. Blagoeva, Anthony J. Kirby, Asen H. Koedjikov, and Ivan G. Pojarlieff

Abstract: The slopes of the pH–rate profiles for the cyclization of 2-methyl- and 2,3-dimethyl hydantoates **1**-NPU and **2**-NPU between pH 1 and 7 change from 1 to 0 and then back to 1. A reaction first order in H^+ was observed with the latter compound. The 2,2,3-trimethyl derivative **3**-NPU showed only one reaction first order in OH^-, but complex acid catalysis is described by slopes 0, –1, 0, and finally –1 again. The cyclizations were general base catalyzed, with Brønsted β values of 0.5–0.6. The OH^- catalysis at higher pH for **1**-NPU and **2**-NPU showed inverse solvent kinetic isotope effects and deviated from the Brønsted relationships, while that for **3**-NPU showed a normal effect and complied with the Brønsted relationship. The accelerations due to the *gem*-dimethyl effect were lost with the OH^- and general base-catalyzed reactions of **3**-NPU. This behaviour is due to a change from the rate-determining formation of the tetrahedral intermediate with **1**-NPU and **2**-NPU to the rate-determining breakdown with **3**-NPU, due to steric hindrance to protonation of the leaving ethoxy group. The OH^- reaction at higher pH involves attack of the ureide anion with **1**-NPU and **2**- NPU, becoming concerted with deprotonation when catalyzed by general bases and changing to acid inhibition of the anion of the tetrahedral intermediate at low pH. With **3**-NPU at higher pH, T^- is in equilibrium and the conjugate acids of the general bases accelerate its breakdown by protonating the ethoxy group. Acid catalysis of the cyclization of **3**-NPU at higher pH is also protonation of the leaving group from T^0 changing to the rate-determining formation of T at lower pH. The latter mechanism is preferred for the cyclization of **2**-NPU.

Key words: *gem*-dimethyl effect, mechanism, general base catalysis, proton transfer, steric hindrance.

Résumé : Les pentes des profils pH–vitesse pour la cyclisation des 2-méthyl- et 2,3-diméthylhydantoates **1**-NPU et **2**-NPU entre les pH 1 et 7 passe de 1 à 0 avant de revenir à 1. Avec le dernier composé, on observe que la réaction est du premier ordre en H^+. Le dérivé 2,2,3-triméthylé **3**-NPU ne donne qu'une réaction du premier ordre en OH^-, mais une catalyse acide complexe décrite par des pentes de 0, –1, 0 et finalement –1 encore une fois. Les cyclisations sont soumises à une catalyse générale par les bases avec des valeurs β de Brønsted qui vont de 0,5 à 0,6. Les **1**-NPU et **2**-NPU soumis à une catalyse par OH^-, à des pH plus élevés, mettent en évidence l'existence d'effets isotopiques cinétiques inverses du solvant et des déviations des relations de Brønsted. Avec OH^-, les accélérations provoquées par l'effet *gem*-diméthyle sont perdues ainsi que les réactions soumises à une catalyse générale par les bases. Ce comportement est dû au fait que dans les cas des **1**-NPU et **2**-NPU l'étape cinétiquement déterminante est la formation d'un intermédiaire tétraédrique alors que dans le cas du **3**-NPU l'étape déterminante est son bris qui est dû à l'empêchement stérique à la protonation du groupe éthoxy partant. La réaction OH^-, à un pH plus élevé, implique une attaque de l'anion uréide par les **1**-NPU et **2**-NPU qui devient concertée avec la déprotonation lorsqu'elle est soumise à une catalyse générale par les bases et qui change à une inhibition acide de l'anion de l'intermédiaire tétraédrique à pH plus bas. Avec le **3**-NPU, à des pH plus élevés, T^- est en équilibre et les acides conjugués des bases générales accélère son bris en protonant le groupe éthoxy. La catalyse acide de la cyclisation du **3**-NPU à des pH plus élevés est aussi la protonation du groupe partant de T^0 qui se change en formation cinétiquement limitante de T à des pH plus faibles. Ce dernier mécanisme est préféré pour la cyclisation du **2**-NPU.

Mots clés : effet *gem*-diméthyle, mécanisme, catalyse générale par les bases, transfert de proton, empêchement stérique.

[Traduit par la Rédaction]

Received December 2, 1998.

This paper is dedicated to Jerry Kresge in recognition of his many achievements in chemistry.

I.B. Blagoeva, A.H. Koedjikov, and I.G. Pojarlieff.[1] Institute of Organic Chemistry, Bulgarian Academy of Sciences, ul. Acad. G. Bonchev block 9, Sofia 1113, Bulgaria.
A.J. Kirby. University Chemical Laboratory, Cambridge CB2 1EW, U.K.

[1]Author to whom correspondence may be addressed. Telephone: +359-2-7334-116. Fax: 359-2-700-225. e-mail: ipojarli@orgchm.bas.bg

Introduction

The hydroxide ion catalyzed cyclization of ethyl 2,2,3-trimethyl-5-phenyl hydantoate, **3**-PUE, is slower than that of the dimethyl compound **2**-PUE (1). This result is surprising because the reaction of **3**-PUE should be subject to the *gem*-dimethyl effect (2): indeed, a normal *gem*-dimethyl effect operates on the acid-catalyzed cyclizations of these compounds (**1**-PUE–**3**-PUE) (3, 4). Data on the general acid-base catalysis and solvent kinetic isotope effects (SKIE) on PUE and their 5-methyl analogues (**1**-MUE–**3**-MUE) led us to the conclusion that the loss of the *gem*-dimethyl effect was due to steric hindrance to proton transfer of the leaving ethoxide group, resulting in a change in the rate-determining step (r.d.s.) from formation to breakdown of the tetrahedral intermediate (3). The balance of evidence as to which r.d.s. is preferred, with the less heavily substituted compounds changing into an alternate one in the fully methylated derivatives, was delicate and thus further evidence was sought for these systems. The improved leaving group ability of the *p*-nitrophenylureido group was intended to bias the system towards rate-determining departure of the ethoxy group, thus allowing a simpler evaluation of the various effects. Grounds for such reasoning were the alternative cyclizations of dicarbamoylglycine **4**: the specific base-catalyzed (SBC) ring closure with the *N*-isopropylcarbamoyl moiety was attributed to r.d. attack of the anion while the GBC reaction involved the end aryl group to r.d. departure of the hydroxy group (5).

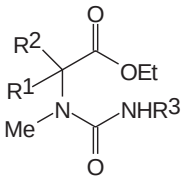

	R^1	R^2		R^3
1	H	H	MUE	Me
2	Me	H	PUE	Ph
3	Me	Me	NPU	4-nitrophenyl

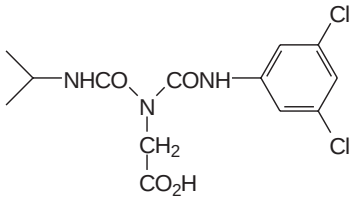

4

Unexpectedly, the hydroxide-catalyzed reaction of the *p*-nitrophenyl esters mirrored the behaviour of the ureido esters with less negative ω-substituents, showing only a small increase in rate with **3**-NPU compared to a large one under acid catalysis, and a normal SKIE opposed to the inverse one with **1**-NPU and **2**-NPU. In contrast to MUE and PUE, however, the *p*-nitrophenyl derivatives showed highly complex rate profiles, varying extensively upon methyl substitution.

We now report how this interplay of the *gem*-dimethyl effect and reaction mechanism can be understood from an analysis of the reaction profiles, general base catalysis, and SKIE. The results obtained support our previous interpretation of the loss of the *gem*-dimethyl effect in the HO^--catalyzed cyclization in esters **3** and allow further insight into the workings of the *gem*-dimethyl effect in reactions through tetrahedral intermediates.

Experimental

Materials

Inorganic reagents and buffer components were of analytical grade and were used without further purification. Potassium hydroxide and buffer solutions were prepared with CO_2-free distilled water. D_2O and DCl (20 wt.% in D_2O), 99 at.% were from Aldrich.

Ethyl esters of methyl substituted 5-(4-nitrophenyl)hydantoic acids were prepared by reaction of the corresponding amino acid esters with 4-nitrophenyl isocyanate. The amino acid esters were converted into the free base form and distilled prior to use. The typical experimental procedure consisted in addition of 10% excess of 4-nitrophenyl isocyanate (3.3 mmol in 5 mL dry benzene) to an ice-cooled solution of the amino acid ester (3 mmol in 5 mL dry benzene). A heavy precipitate was formed immediately and the reaction mixture was left for 20 min at room temperature. The precipitated product was filtered, washed with dry benzene, and dried in a vacuum desiccator with P_2O_5. The products could not be heated or recrystallized due to their fast cyclization at higher temperatures. **3**-NPU cyclized readily in the presence of traces of moisture and was best stored in sealed ampoules at low temperatures. The purity of the products was checked by NMR and the yields of pure esters were 62–64%.

*Ethyl 3-methyl-5-(4-nitrophenyl)hydantoate (**1**-NPU)*: mp 124–125°C. IR $\nu_{max}(CHCl_3)/cm^{-1}$: 1727 (CO ester), 1676 (CO ureido). ^1H NMR ($CDCl_3$) δ (ppm): 1.31 (t, *J* 7.1 Hz, 3H, CH_3CH_2), 4.15 (s, 2H, N-CH_2), 3.16 (s, 3H, CH_3N), 4.25 (q, *J* 7.1 Hz, 2H, CH_2O), 7.08 (s, 1H, HN), 7.54–8.19 (m, 4H, Ar).

*Ethyl 2,3-dimethyl-5-(4-nitrophenyl)hydantoate (**2**-NPU)*: mp 130–131°C. IR $\nu_{max}(CHCl_3)/cm^{-1}$: 1727 (CO ester), 1672 (CO ureido).^1H NMR (CDCl) δ (ppm): 1.30 (t, *J* 7.2 Hz, 3H CH_3CH_2), 1.49 (d, *J* 7.35 Hz,, 3H CH_3CH), 3.04 (s, 3H, CH_3N), 4.23 (q, *J* 7.2 Hz, 2H, -CH_2O), 5.04 (q, *J* 7.35 Hz 1H,-CHN), 6.99 (s, 1H, HN), 7.56–8.20 (m, 4H, Ar).

*Ethyl 2,2,3-trimethyl-5-(4-nitrophenyl)hydantoate (**3**-NPU)*: mp 125–127°C. IR $\nu_{max}(CHCl_3)/cm^{-1}$: 1725 (CO ester), 1670 (CO ureido). ^1H NMR (CDCl) δ (ppm): 1.29 (t, *J* 7.1 Hz, 3H, CH_3CH_2), 1.51 (s, 6H, $(CH_3)_2C$), 3.07(s, 3H, CH_3N), 4.21 (q, *J* 7.1 Hz, 2H, CH_2O), 7.28 (s, 1H, HN), 7.49–8.34 (m, 4H, Ar).

Product analysis

The cyclizations of the ethyl hydantoates studied in this paper proceeded quantitatively to the corresponding hydantoins. Good isosbestic points were obtained for all three compounds studied and the end-point absorbances for the kinetic runs were identical within experimental error with the absorbances of model solutions of the respective hydantoins described previously (6).

Kinetic measurements

Rate constants were determined at 25.0 ± 0.01°C under pseudo-first-order conditions in the thermostatted cell com-

Fig. 1. Rate profiles for the cyclization of **1**-NPU (○) and **2**-NPU (△).

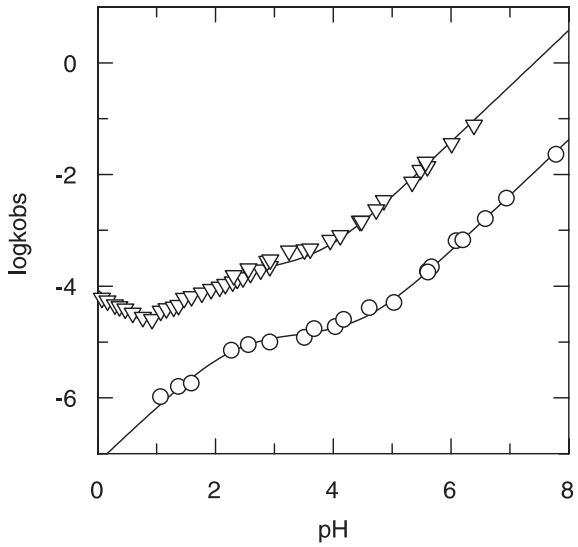

partment of a Unicam SP-800 spectrophotometer. The rates of cyclization of the substituted esters were followed by monitoring the decrease of the absorbance at 330 nm due to the 4-nitrophenylureido group. Reactions were initiated by injecting 20 mL of 1×10^{-2} M stock solutions of the substrates in dry THF into 2.7 cm^3 of preheated buffer solution. Ionic strength was maintained constant (1.0 M) with KCl. Measurements of pH values and calculations of the observed pseudo-first-order rate constants (k_{obs}) were as previously described (7). Good linear plots ($r > 0.999$) of $\ln(A_t - A_\infty)$ against time were obtained over three half-lives and k_{obs} values were reproducible to within 3% with the exception of the slow ring closure of **1**-NPU in hydrochloric acid below pH 2 where the hydrolysis of the ester group was significant. Since the product acids cyclized more rapidly than the esters, plots of $\ln(A_t - A_\infty)$ against time sloped downwards with time. In this case the rate constants were obtained from the initial part of the reaction where linearity was preserved: initial rates in 0.1 M Hcl up to ca. 20% conversion in 0.01 M HCl.

Solvent kinetic isotope effects

The solvent kinetic isotope effects (SKIE) for k_H were determined by comparison of k_{obs} values measured in solutions of HCl or DCl of the same concentration. The k_{OH} values for calculation of SKIE were determined by extrapolation to zero buffer concentrations of k_{obs} in phosphate or cacodylate buffers both in H_2O and D_2O. For the hydroxide-catalyzed reaction k_0 values were divided by the activity of HO^- or DO^- to obtain k_{OH} or k_{OD}. pD values were obtained by adding 0.4 to the pH-meter readings and the a_{OD} values were calculated using $pK_w = 14.86$ (8).

Results and discussion

Rate profiles

1. Base catalysis

With ureido ester **1**-NPU the slope of the plot of log k_{obs} versus pH changes from 1 to 0 and then back again to 1 (Fig. 1).

Fig 2. Rate profile for the cyclization of **3**-NPU.

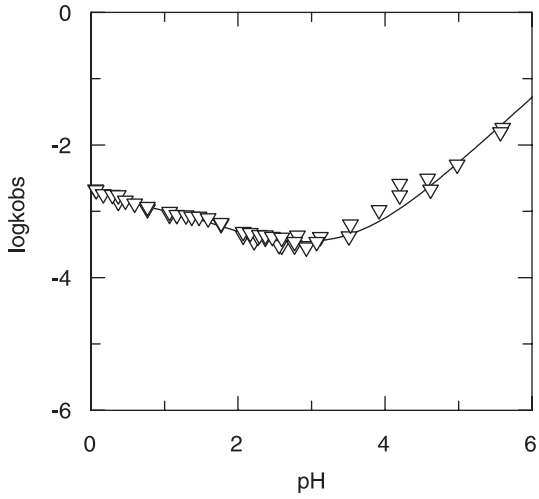

Scheme 1.

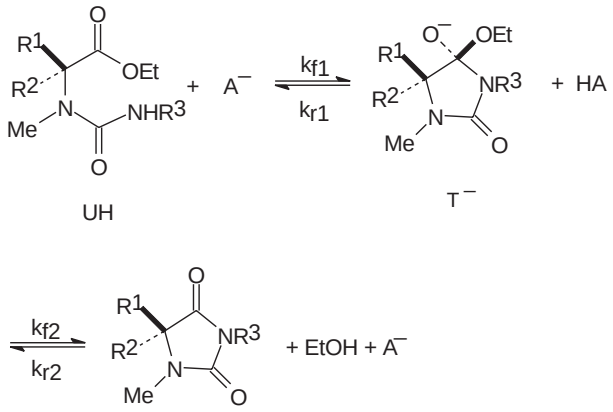

Below pH = 1, hydrolysis of the ester group was observed and acid catalysis could not be detected. With the faster cyclization of compound **2**-NPU the reaction could be studied up to 1 M HCl and an acid-catalyzed region could be registered in addition to base catalysis. The latter is also best described by equations leading to the same changes of slopes against pH, from 1 to 0 and back again to 1. The minimum between the acid-catalyzed and base-catalyzed regions occurs around pH = 1, illustrating the very poor nucleophilicity of the neutral *p*-nitrophenylureido group. The same minimum occurs around pH 3 with **2**-PUE (3).

The behaviour of ester **3**-NPU, presented separately in Fig. 2 to avoid overlap in the base-catalyzed region, is distinctly different: only one segment, first order in $[OH^-]$, is observed, while the acid catalysis region is complex.

The rate law for base catalysis can be derived from Scheme 1, depicting the main steps in the reorganization of bonds from reactants to products.

The steady state solution is

$$[1] \qquad k_{obs} = \frac{k_{f1}[A^-]k_{f2}[HA]}{(k_{r1} + k_{f2})[HA]}$$

When the bases are water and hydroxide ion this becomes

Table 1. Kinetic solvent isotope effects for ring closure of methyl substituted ethyl 5-(4-nitrophenyl)hydantoates at 25°C

Substrate	[LCl] mol dm^{-3}	$(k_H / k_D)_{obs}$	pH (H)	k_{OH} / k_{OD}
1-NPU	0.002	2.9	5.60[a]	0.78
	0.005	2.4		
	0.01	1.8		
2-NPU	0.005	3.0	5.57[b]	0.6
	0.01	2.9		
	0.90	0.8		
3-NPU	0.005	2.5	5.62[b]	1.8
	0.01	2.6	5.82[c]	1.9
	0.90	1.1		

[a]Cacodylate buffer 20% base.
[b]Phosphate 10% base.
[c]Phosphate 15% base.

$$[2] \qquad k_{obs} = \frac{(k_{f1w} + k_{f1OH}[OH^-])(k_{f2w} + k_{f2H}[H^+])}{k_{r1w} + k_{f2w} + (k_{r1H} + k_{f2H})[H^+]}$$

*1(a). Ethyl hydantoates **1**-NPU and **2**-NPU*: Various limiting conditions lead to simplified forms of eq. [2], describing rate profiles with slopes changing from 1 to 0 and then back to 1. In the following discussion[2] we designate the apparent second-order constant at lower pH as $k_{OH}{}^a$ and the one at higher pH as $k_{OH}{}^b$. Two conditions have to be met (9) in order that two different k_{OH} are observed in situations described by eq. [2]. The first is that the two forward fractions for breakdown of T^-, $k_{f2}/(k_{r1} + k_{f2})$, for H_2O and H^+ catalysis, respectively, have to be different. The first one will operate at higher pH and the second one at lower pH. Two different reactions of the same order are usually associated with a change in the rate-determining step; in the case under discussion, when $k_{r1w} < k_{f2w}$ then $k_{r1H} > k_{f2H}$ or vice versa. The second condition for two reactions of the same order to be observed is that the intermediates involved should not equilibrate. In such a case the reactions go simply by the lowest energy path available to, for example, T^-, which in turn corresponds to single first order in the $[OH^-]$ region in the rate profile. In our case two different k_{OH} can be observed when one or both processes are general acid–base catalyzed.

As is generally the case for kinetically equivalent mechanisms, the preference must be based on non-kinetic evidence. Comparison of the rate profiles of Figs. 1 and 2 with the SKIE data listed in Table 1 shows that the $k_{OH}{}^a$ values for **1**-NPU and **2**-NPU, as well as the single k_{OH} constant for **3**-NPU, exhibit normal isotope effects ($k_H > k_D$) These allow a choice between various possible mechanisms. The similarity in the p*K*'s of the *p*-nitrophenylureido group and water, the conjugate acid of OH^-, could give rise to a normal SKIE (10) for proton removal from nitrogen (a p*K* of 14 has been reported for *p*-nitrophenylurea (11)). However, if this step was rate determining, a Brønsted β value of 1 is expected, contrary to the observed values of 0.5–0.6 (vide infra Table 6). Such a deprotonation would be diffusion controlled and would certainly be much faster than the overall rates in at least two of the cases; second-order constants of ca. 10^6–10^7 dm^3 mol^{-1} s^{-1} are observed for the $k_{OH}{}^a$ of **1**-NPU and for the k_{OH} of **3**-NPU (Table 2). Participation of OH^- in a concerted process in which the N—C bond is formed while the NH proton is pulled off (formula **5**, B = OH^-) is also unlikely because, according to the libido rule of Jencks (12), the base has to be of strength intermediate between that of the proton-donating group in the ground and product states. The alternative SB-GAC mechanism for N—C formation, i.e., attack of the ureide anion concerted with proton transfer

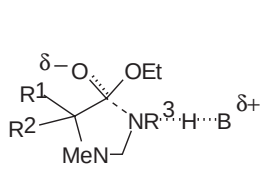

5

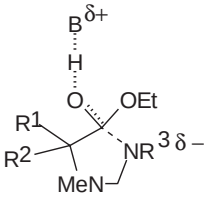

6

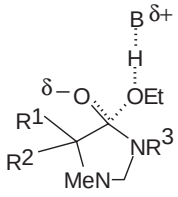

7

to the ester carbonyl leading to T^0 (formula **6**, B = OH^-) was refuted (3) for the ω-methyl and ω-phenyl analogues MUE and PUE as it contradicts Jencks' requirement for T^- to be an unstable intermediate (13); this apparently applies also for NPU to permit the SBC catalyzed reaction of **1**-NPU and **2**-NPU presented by $k_{OH}{}^b$, discussed below. We are thus left with the last possible proton transfer as the cause of the normal SKIE, that is, water donating a proton to the ethoxy group cleaving from T^- (formula **7**, B = OH^-). As discussed before (3), a concerted mechanism is possible with a late C—O bond cleavage. In terms of Scheme 1 and eq. [2], this mechanism requires $k_{r1} > k_{f2}$. The process $k_{OH}{}^a$ is observed at low pH when $k_{r1w} + k_{f2w} < (k_{r1H} + k_{f2H})[H^+]$ so the inequality $k_{r1H} > k_{f2H}$ will apply. When $k_{f1w} > k_{f1OH}[OH^-]$ and if $k_{f2w} > k_{f2H}[H^+]$ in the region for base catalysis, the observed rate constant becomes

$$[3] \qquad k_{obs} = \frac{k_{f1w}k_{f2w}}{k_{r1H}[H^+]}$$

The rate constant first order in $[OH^-]$ at low pH can be then be presented as

$$[4] \qquad k_{OH}^a = \frac{K_{T^-}k_{f2w}}{K_w}$$

where k_{T^-} is the equilibrium constant for formation of T^- when $A^- = H_2O$. Thus at low pH the first order in $[OH^-]$ behaviour is determined by the equilibrium concentration of T^-, and the rate-determining step is the water-catalyzed decomposition of T^-. Such a mechanism is referred to as acid inhibition of T^- (14).

[2]For the sake of brevity exhaustive consideration of the various cases afforded by eq. [2] will be avoided.

Table 2. Rate constants for H^+, OH^-, and H_2O catalyzed ring closure of ethyl 5-(4-nitrophenyl)hydantoates at 25°C and ionic strength 1.0 M.

Compound	k_{OH}[b] $dm^3\ mol^{-1}\ s^{-1}$	k_{OH}[a] $dm^3\ mol^{-1}\ s^{-1}$ [b]	$k_w\ s^{-1}$	$k_{2H}\ dm^3\ mol^{-1}\ s^{-1}$	$k_{1H}\ dm^3\ mol^{-1}\ s^{-1}$
1-NPU[a]	(4.23±0.22) × 10^4	(6.94±0.69) × 10^6	(1.36±0.11) × 10^{-5}	196±30	
2-NPU[c]	(3.85±0.20) × 10^6	(2.07±0.019) × 10^8	(2.18±0.16) × 10^{-4}	107±16	(8.34±0.61) × 10^{-5}
	k_{OH}	$k_{1w}\ s^{-1}$	$k_{2w}\ s^{-1}$		
3-NPU[d]	(5.20±0.37) × 10^6	(1.10±0.18) × 10^{-3}	(2.46±0.37) × 10^{-1}	35.2±16.9	(1.21±0.36) × 10^{-3}

[a]Equation [5].
[b]$k_w / k_{2H}K_w$.
[c]Equation [6].
[d]Equation [12].

Scheme 2.

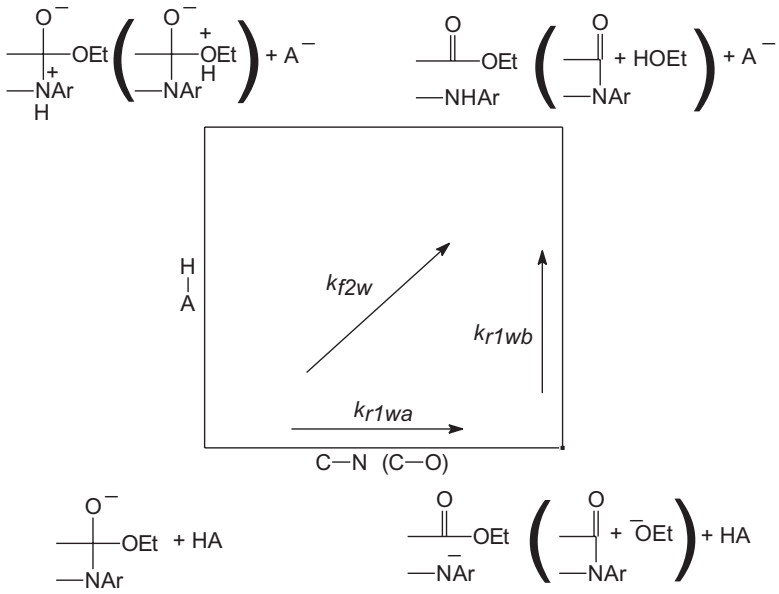

Upon increasing the pH, the plateau is reached with **1**-NPU and **2**-NPU when the $[H^+]$ term in the denominator can be neglected. Now $k_{obs} = k_{f1w}$ because, as discussed above, $k_{r1w} < k_{f2w}$ in order for the second slope of 1 in the rate profile to be observed at higher pH. Then $k_{obs} = k_{f1OH}[OH^-]$. With the above limitations eq. [2] can be simplified to

$$[5] \qquad k_{obs} = \frac{k_w + k_{OH}[OH^-]}{1 + k_{2H}[H^+]}$$

where $k_{OH} = k_{OH}^b = k_{f1OH}$, $k_w = k_{f1w}$, $k_{2H} = k_{r1H}/k_{f2w}$, and $k_{OH}^a = k_w/(k_{2H}K_w)$. The rate constants for **1**-NPU in Table 2 were obtained by fitting the rate data to eq. [5]. In the case of **2**-NPU the equation was expanded with a term for acid catalysis.

$$[6] \qquad k_{obs} = \frac{k_w + k_{OH}[OH^-]}{1 + k_{2H}[H^+]} + k_{1H}[H^+]$$

The $k_{OH}{}^b$ constants for **1**-NPU and **2**-NPU refer to an SBC process as evidenced by the inverse isotope effect at pH = 5.6 where, according to Fig. 1, the second first order in $[OH^-]$ process dominates. Because, as already discussed, $k_{r1w} < k_{f2w}$, this is r.d. formation of T^- taking place by preliminary ionization of the ureido esters.

The crossover of reactivities for H_2O and H_3O^+ catalysis of partitioning of the intermediate is an interesting problem. The inequality $k_{r1w} < k_{f2w}$ means that *p*-nitrophenylureido leaves less readily than ethoxide at high alkalinity against expected fugacities while the opposite is true at low pH ($k_{r1H} > k_{f2H}$). The reason for the former inequality can be sought in reactivities of stepwise vs. concerted processes (15). The acid-catalyzed breakdown of T^- can be described by the alternate route diagram (16) shown in Scheme 2. When HA = H_2O, the leaving of the ureido group is a two-step process along the edges of the diagram: splitting off of the ureide anion, $k_{r1w}{}^a$, followed by proton transfer from H_2O to the nitrogen atom, $k_{r1w}{}^b$. This is not a concerted process for reasons discussed above explaining why OH^- cannot act as a general base in the reverse reaction and, in terms of the alternate route diagram, this happens because the energy of the bottom right-hand corner is considerably lower than that of the top-left corner. On the other hand, as discussed above for **3**-NPU, the ethoxy group cleaves along the diagonal in a one-step process with both bonds changing simultaneously, k_{f2w}. This occurs because the energy of the bottom-right corner is raised, ethanol being a weaker acid by more than two p*K* units, and that of the top-left corner is lowered because of the greater basicity of the ethoxy group. Thus a valley along the diagonal is created, with the energy of the transition state apparently lower than that for the attack of the ureide anion.

When HA = H_3O^+ the relationships in the diagram change significantly. Considered in the reverse direction, the

Scheme 3.

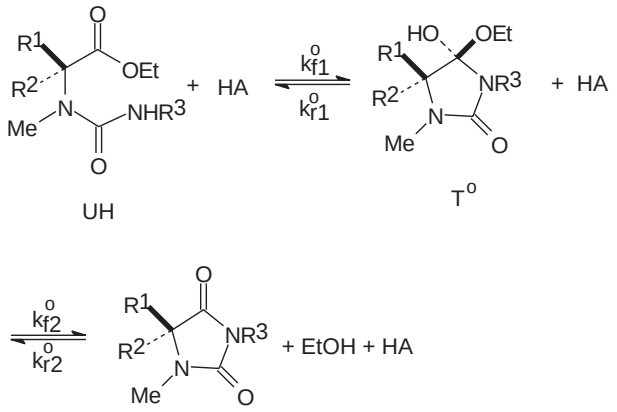

deprotonation by water along the right-hand edge is now quite an uphill reaction, offering no easy bypassing of the zwitterions at the top-left corner. These are highly unstable and so will enforce general catalysis. This applies to both reactions, k_{r1H} and k_{f2H} and, when the mechanism is the same, the intrinsically better fugacity of the *p*-nitrophenylureido group determines reactivity.

*1(b). Ethyl hydantoate **3**-NPU*: In contrast to **1**-NPU and **2**-NPU, the rate profile of **3**-NPU (Fig. 2) is characterized by a single rate constant first order in [OH^-]. This implies that the partitioning ratios for water and H^+ catalyzed breakdown of T^- of **3**-NPU are biased in the same way, i.e., no change in the r.d.s. takes place. Why **3**-NPU is different can be understood by comparing with previous results on MUE and PUE (3). The inverse SKIE observed with the $k_{OH}{}^b$ constants for **1**-NPU and **2**-NPU and the normal effect with the k_{OH} constant for **3**-NPU repeat the pattern of **1**–**3**-MUE and PUE. Significant also is the disappearance of the *gem*-dimethyl effect with the k_{OH} of **3**-NPU: in contrast to acid catalysis, where **3**-NPU reacts 15 times faster than **2**-NPU, the rates in the higher pH region are almost the same (Table 2). The change of mechanism brought about by the introduction of the extra methyl group in **3**-MUE or **3**-PUE was explained by steric hindrance to protonation of the oxygen atom of the ethoxy group. The ester ethyl group will adopt the least crowded conformation, blocking easy protonation of the ethoxy oxygen because its lone pairs are effectively shielded in a half-chair conformation by the methyl groups on C-5 and the aryl ring on N-2 (see **8**; for clarity, one of the methyl groups at C-5 in the formula is represented by a single bond).

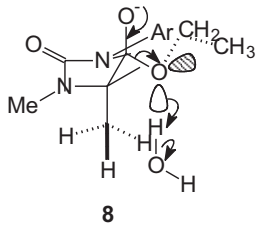

8

Thus there is good reason to believe that, for **3**-NPU, steric hindrance to protonation determines r.d. breakdown of T^-, concerted with catalysis by water. When the ethyl group is replaced by hydrogen, as is the case with the respective hydantoic acids, the intermediate becomes less crowded and slowing down is no longer observed.[3] The GBC cyclization of thioureido esters (17) and the above-mentioned (5) GBC cyclization of the aryl moiety of the *N*,*N*-dicarbamoylglycine **4** are also believed to be limited by breakdown of T^-.

2. Acid catalysis

The complex course for acid catalysis of the cyclization of **3**-NPU can be accommodated by an equation predicting four regions of slopes 0, –1, 0, and –1 in the rate profile on decreasing pH. Such an equation can be derived from Scheme 3, similar to Scheme 1, involving H^+ and water-catalyzed formation and decomposition of T^0.[4] This would then yield an equation in the format of eq. [2], the superscripts 0 denoting that they are related to T^0.

$$[7] \qquad k_{obs} = \frac{(k^0_{f1w} + k^0_{f1H}[H^+])(k^0_{f2w} + k^0_{f\,2H}[H^+])}{(k^0_{r1w} + k^0_{f\,2w}) + (k^0_{r1H} + k^0_{f\,2H})[H^+]}$$

To describe the rate profile for acid catalysis we chose the combination $k^0_{r1w} > k^0_{f\,2w}$ and $k^0_{r1H} < k^0_{f2H}$ because when [T^-] reaches equilibrium (as assumed in the preferred mechanism for k_{OH} of **3**-NPU) so should [T^0] and the constants for water catalysis are important in the overlapping region. So when all the [H^+] terms are small one gets

$$[8] \qquad k_{obs} = \frac{k^0_{f1w}k^0_{f\,2w}}{k^0_{r1w} + k^0_{f\,2w}} \approx K_{T^0}k^0_{f\,2w}$$

Equation [8], the water-catalyzed decomposition of T^0, is kinetically equivalent to another pathway: the H^+-catalyzed decomposition of T^-, $k_{obs} = K_{T-}\,k_{f2H}$, and the latter is most probably a more efficient one.

After the plateau described by eq. [8], most likely the adjoining slope of –1 is due to acid-catalyzed decomposition of T^0:

$$[9] \qquad k_{obs} = K_{T^0}k^0_{f2H}[H^+]$$

followed by a change in the rate-determining step when $(k^0_{r1w} + k^0_{f2w}) < (k^0_{r1H} + k^0_{f2H})[H^+]$:

$$[10] \qquad k_{obs} = k^0_{f1w}$$

This formally acid-catalyzed reaction according to Scheme 3 is also most likely the kinetically equivalent general base catalysis by water.

Finally, when $k_{f1w} < k_{f1H}[H^+]$

$$[11] \qquad k_{obs} = k^0_{f1H}[H^+]$$

The rate profile can then be described by eq. [12]:

$$[12] \qquad k_{obs} = \frac{(k_{1w} + k_{1H}[H^+])(k_{2w} + k_{2H}[H^+])}{1 + k_{2H}[H^+]} + k_{OH}[OH^-]$$

$$k_{OH} = \frac{k_{T^-}k_{f2w}}{K_w};\ k_{2w} = K_{T^-}k_{f2H} \text{ or } = K_{T^0}k^0_{f2w};\ k_{2H} = K_{T^0}k^0_{f2H};$$
$$k_{1w} = k^0_{f1w};\ k_{1H} = k^0_{f1H}.$$

[3] To be published.

[4] Catalysis by H^+ can be formally assumed to produce T^o as T^+ loses proton to bulk water under diffusion control.

Fig. 3. Plot of k_{buf} against fraction base in acetate buffers for **2**-NPU.

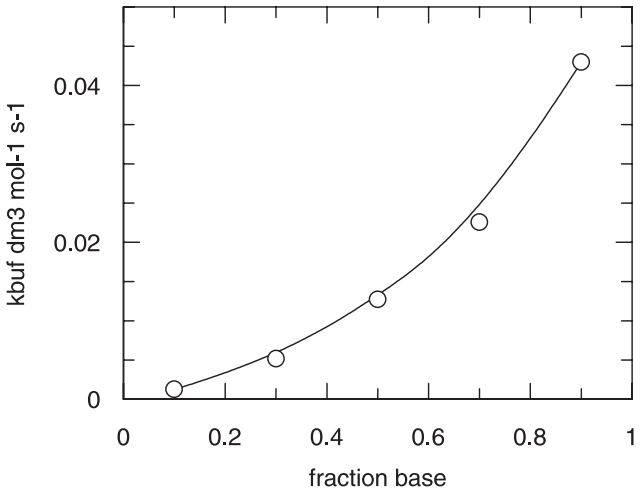

The above assignments of mechanism agree well with the SKIE values listed in Table 1. In 0.90 M LCl it is 0.8 for **2**-NPU. This value applies for a "clean" reaction and is the same as the values of 0.7–0.8 found for ω-phenylhydantoic esters.(4) This and other evidence with the latter (4) supported rate-determining formation of T via the transition state **9**:

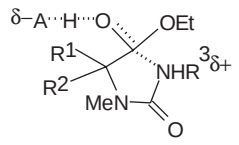

9

The somewhat larger SKIE value of 1.1 for **3**-NPU does not contradict the conclusion for k_{f1H} as rate determining at the highest acidity because it is most probably enlarged by contribution from the water-catalyzed reaction. According to Table 1, effects of about 2.5–3 are observed at lower [LCl] with **2**-NPU and **3**-NPU.

3. General base catalysis

In contrast to the case of ω-phenylureido esters where GC was clearly expressed only in the case of **3**-PUE and difficult to establish with the remaining compounds, the effect of buffer catalysis was significant and could be readily monitored with all three *p*-nitrophenylureido derivatives.

Corrections for buffer failure were carried out as pH varied strongly at low fractions of base in acid phosphate and glycine buffers. Changes in pH were satisfactorily reproduced by solving the equation for the ionization

$$K_{AH} = \frac{(C_A - a_H)a_H}{(C_{AH} + a_H)}$$

where K_{AH} is the dissociation constant at I = 1 M KCl according to ref. 7, C_A and C_{AH} are the concentrations as weighed, and the actual concentration of the buffer components may be approximated as $[A^-] = C_A - a_H$, and $[AH] = C_{AH} + a_H$.

Fig. 4. Plot of k_{buf} against fraction base for **1**-NPU in neutral phosphate. Insert excluding data for 0.9 fraction base.

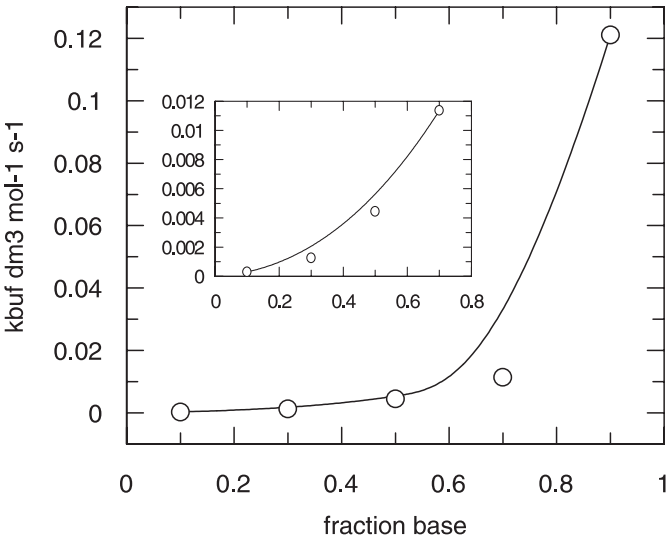

Plots of k_{buf} vs. fraction (of) base were convex to a varying degree. The "nonlinear" behaviour is illustrated by the examples in Figs. 3 and 4.

This nonlinearity is appreciable when a wide range of buffer ratios are studied. With narrow ranges it is indicated by the negative intercepts in plots of k_{buf} vs. fraction base. A solution was sought by means of equations derived from Scheme 1. When a general base is included in Scheme 1, the full steady state treatment yields a complex solution that can reasonably be analyzed only under simplifying assumptions. The constants for general base catalysis were obtained by nonlinear regression curve fitting of the equations shown below. The parameters describing the rate profile as a function of pH were fed in as known constants. A series of equations were tried: only those that gave good fits will be discussed. Unless stated otherwise, all equations used have a $1 + k_{2H}[H^+]$ term in the denominator; k_{2H} from the rate profiles (Table 2) varies from around 200 in **1** to 30 in **3**, which means that at pH > 3 its influence becomes negligible.

In cases when the general base is HPO_4^{2-} we found previously (3) that upward trends at high buffer ratios are described well by the addition of a $k_{BOH} \times [B] \times [OH^-]$ term interpreted as PO_4^{3-} catalysis. An extensive series of data in neutral phosphate for ester **1** was treated by means of eq. [13]:

$$[13] \qquad k_{obs} = \frac{k_w + k_{OH}[OH^-] + k_B[B] + k_{BOH}[OH^-][B]}{1 + k_{2H}[H^+]}$$

(The k_H term is negligible in neutral phosphate.) This equation gave the very good fit as illustrated in Fig. 5, which compares the experimental with the calculated points (eq. [14] is a multivariable function and cannot be presented as a two-dimensional graph).

The rate constant for catalysis for PO_4^{3-} is obtained as $k_{PO_4^{3-}} = k_{BOH}K_w/K_{HPO_4^{2-}}$.

Alternately the deviations from linearity could be described by equations including a k_{BH} term in the denominator. The following two equations proved most useful with

Table 3. Buffer catalysis data for the cyclization of ethyl 3-methyl-5-(4-nitrophenyl)-hydantoate, **1**-NPU, at 25°C and ionic strength 1.0 M.

Buffer acid	pK_{AH}[a,b]	Conc. range mol dm^{-3}	Runs	% base	10^4 k_B dm^3 mol^{-1} s^{-1}[b]	10^4 $k_{2BH}(k_{1BH})$ dm^3 mol^{-1} s^{-1}
H_3O^+	–1.74				0.136 ± 0.011[c]	
	(–1.26)					
$H_3N^+CH_2CO_2H$	2.45	0.1–0.5	3	30	0.274 ± 0.067[d]	27 000 ± 18 000
		0.1–0.5	3	50		(0.32 ± 0.17)
		0.1–0.5	3	70		
		0.1–0.5	3	90		
HCO_2H	3.57	0.01–0.5	4	50	2.77 ± 0.13[d]	21 500 ± 2600
		0.01–0.5	4	70		(0.432 ± 0.189)
CH_3CO_2H	4.62	0.1–0.5	4	30	7.28 ± 0.19[e]	5000 ± 2.9800
		0.1–0.5	4	50		
		0.1–0.5	4	70		
$(CH_3)AsO_2H$	6.19	0.01–0.3	4	20	56.7 ± 2.8[f]	
		0.01–0.3	4	30		
		0.01–0.4	5	50		
$H_2PO_4^-$	6.48	0.016–0.2	4	10	42.7 ± 3.1[g] (21.3)	
		0.016–0.5	4	30		
		0.016–0.5	9	50		
		0.016–0.4	8	70		
		0.016–0.35	5	90		
HPO_4^{2-}	12.32				978 000[h]	
	(11.84)				(326 000)	
H_2O	15.74				(4.23 ± 0.22) × 10^8	
	(16.04)					

[a] pK_{AH} values from ref. 7.
[b] Statistically corrected values in parentheses.
[c] First-order rate constant.
[d] Equation [15].
[e] Equation [14].
[f] Equation [5] + k_B[B].
[g] Equation [13].
[h] Calculated from k_{BOH}.

compounds **1**-NPU and **2**-NPU. They derive from eq. [1] under certain conditions.

$$[14] \quad k_{obs} = \frac{k_w + k_{OH}[OH^-] + k_B[B]}{1 + k_H[H^+] + k_{2BH}[BH^+]}$$

$$[15] \quad k_{obs} = \frac{k_w + k_{OH}[OH^-] + k_B[B] + k_{1BH}[BH^+]}{1 + k_H[H^+] + k_{2BH}[BH^+]}$$

In the case of ester **2**-NPU the term for H^+ catalysis was added as in eq. [6].

Equation [14] is an extension of eq. [5], derived by assuming that k_{BH} behaves as k_{2H} in the case of **1** and **2**, that is, $k_{r1BH} > k_{f2BH}$ and $k_{f2BH}[BH^+] < k_{f2w}$ in the range studied. Then $k_B = k_{f1B}$ and $k_{2BH} = k_{r1BH}/k_{f2w}$ ($k_{f2w} > k_{r1w}$). The increase of $k_{2BH}[BH^+]$ with the decrease of fraction base will cause at the same time $_{kbuf}$ to decrease faster than demanded by a linear function. These assumptions mean that k_B is involved in the formation of T^- and can be measured directly as long as formation of T^- is r.d. for the overall reaction. When k_{2BH} $[BH^+]$ becomes greater than $1 + k_H[H^+]$ there is a change in the r.d.s.; actually eq. [14] predicts reaching the situation determined by eqs. [3] and [4], the first step becoming an equilibrium and T^- giving products by k_{f2w}.

Fig. 5. Logarithms of the first-order rate constants for cyclization of **1**-NPU in neutral phosphate: (○) experimental data, (●) theoretical points obtained by means of eq. [14] and parameters in Tables 2 and 3.

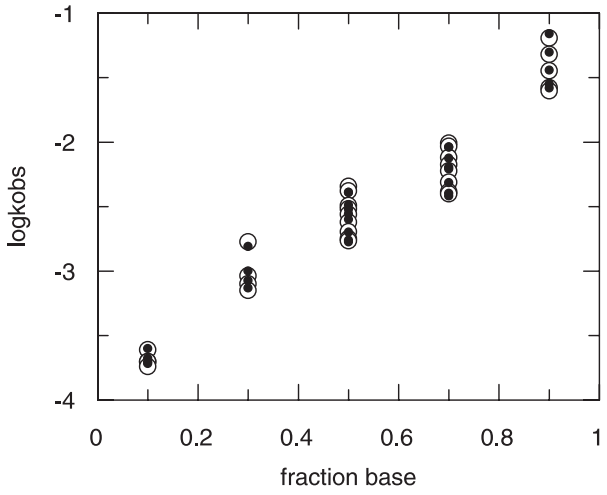

Equation [15] improves the fit further in some cases. The term k_{1BH} $[BH^+]$ in the numerator could either be due to

Table 4. Buffer catalysis data for the cyclization of ethyl 2,3-dimethyl-5-(4-nitrophenyl)-hydantoate, **2**-NPU, at 25°C and ionic strength 1.0 M.

Buffer acid	pK_{AH} [a,b]	Conc. range mol dm^3	Runs	% base	10^4 k_B dm^3 mol^{-1} s^{-1} [a,b]	10^4 k_{2BH} dm^3 mol^{-1} s^{-1}
H_3O^+	–1.74				2.18 ± 0.16[c]	
	(–1.26)					
H_3PO_4	1.78	0.01–1	6	30	16.1 ± 2.0[d]	120 000 ± 21 300
	(2.26)	0.01–1	6	50		
		0.1–1	5	70		
		0.1–1	5	90		
$H_3N^+CH_2CO_2H$	2.45	0.1–1	3	50	12.7 ± 1.3[d]	22 400 ± 5500
		0.1–1	3	70		
		0.1–1	3	90		
HCO_2H	3.57	0.01–0.2	4	30	65.9 ± 5.6[e]	
		0.01–0.2	4	50		
		0.01–0.2	4	70		
		0.01–0.2	4	90		
CH_3CO_2H	4.62	0.05–0.2	3	10*	533 ± 64[d]	78 800 ± 19 100
		0.01–0.2	4	30		
		0.01–0.2	4	50		
		0.01–0.2	4	70		
		0.05–0.2	3	90		
$(CH_3)AsO_2H$	6.19	0.01–0.15	4	10	1930 ± 170[e]	
		0.01–0.15	4	20		
		0.01–0.15	4	30		
		0.01–0.15	4	50		
		0.01–0.15	4	70		
H_2O	15.74				(3.85 ± 0.20) × 10^{10}	
	(16.04)					

[a] pK_{AH} values from ref. 4.
[b] Statistically corrected values in parentheses.
[c] First-order rate constant.
[d] Equation [14].
[e] Equation [6] + k_B[B].

$k_{f2BH}[BH^+]$ not being negligible in eq. [1] and result from $k_{f1w} \times k_{f2BH}$. Independent GAC is another possibility.

However, within the experimental data available for compounds **1** and **2**, a definite choice cannot be made between eqs. [14] and [15]. Equation [15] performed better with **1**-NPU but there is no considerable improvement over eq. [14]. In contrast,with ureido ester **2**-NPU eq. [14] is definitely the better choice as eq. [15] fails. With the stronger buffer bases, acid catalysis becomes unimportant. In acetate and cacodylate buffers, either a straightforward equation for GBC (adding kB × [B] to eqs. [5] or [12]) best described the results or the more complex equations gave insignificant improvement together with unrealistic additional constants.[5]

For compound **3**-NPU the following modification of eq. [12] was preferred in the case of the more acidic buffers such as acid phosphate, glycine, and formate (the latter gave large errors for the BH constants):

$$[16]\quad k_{obs} = \frac{(k_{1w} + k_{1H}[H^+])(k_{2w} + k_{2H}[H^+]) + k_B[B] + k_{1BH}[BH^+]}{1 + k_{2H}[H^+] + k_{2BH}[BH^+]} + k_{OH}[OH^-]$$

The data obtained in acetate were best described by an equation assuming independent GBC. In cacodylate and neutral phosphate only a few measurements at low fraction base could be taken due to the fast reaction and the rate constants were obtained by assuming independent GBC.

The rate constants for GBC listed in Tables 3–5 yield the Brønsted plots shown in Fig. 6. The lines drawn are linear fits obtained from the data for the general bases with pK's between 2 and 6.5. The data for ureido ester **3**-NPU in acid phosphate and glycine buffers deviate strongly from the Brønsted plot and the β-value was determined from the remaining four data points. The slopes of the lines are presented in Table 6. As observed before for the cyclization of ethyl 5-phenylhydantoates, the points for water catalysis fall on the correlation lines. It is noteworthy that the data for OH^- catalysis repeat the pattern observed with the ω-methyl and ω-phenyl analogues of compounds **1**-NPU–**3**-NPU. Esters **1**-NPU and **2**-NPU exhibit strong positive deviations while the point for **3**-NPU fits the line, a behaviour parallel to the SKIE results.

The present series of Brønsted linear relationships for three NPU hydantoates with increasing numbers of methyl groups revealed an unexpected feature: the *gem*-dimethyl effect on

[5] It should be noted also that eq. [13] on the one hand and eqs. [14] and [15] on the other give different k_B constants in principle. With eq. [13] k_B is approached at low [OH^-], while with eqs. [14] and [15] k_B is approached at high [OH^-] (low [BH^+]).

Table 5. Buffer catalysis data for the cyclization of ethyl 2,2,3-trimethyl-5-(4-nitrophenyl)-hydantoate, **3**-NPU, at 25 °C and ionic strength 1.0 M.

Buffer acid	pK_{AH} [a,b]	Conc. range mol dm^3	Runs	% base	$10^4 k_B$ dm^3 mol^{-1} s^{-1} [b]	$10^4 k_{2BH}(k_{1BH})$ dm^3 mol^{-1} s^{-1}
H_3O^+	–1.74 (–1.26)				11.0 ± 1.8[c]	
H_3PO_4	1.78 (2.26)	0.01–1	6	30	492 ± 104[d]	73 700 ± 44 200
		0.01–1	6	50		(992 ± 426)
		0.1–1	5	70		
		0.1–1	5	90		
$H_3N^+CH_2CO_2H$	2.45	0.1–1	3	30	759 ± 134[d]	60 100 ± 26 100
		0.1–1	3	50		(518 ± 258)
		0.1–1	3	70		
		0.01–1	4	90		
HCO_2H	3.57	0.1–0.5	4	30	165 ± 7.2[d]	3350 ± 2880
		0.1–0.5	4	50	172[e]	(16.3 ± 6.2)
		0.1–0.5	4	70		
CH_3CO_2H	4.62	0.01–0.5	9	30	1190 ± 40[e]	
		0.01–0.5	9	50		
		0.01–0.2	4	70		
$(CH_3)AsO_2H$	6.19	0.01–0.3	4	20	17 500 ± 1500 [f]	
$H_2PO_4^-$	6.48	0.008–0.2	8	10	14 900 ± 5100 [f]	
		0.008–0.048	4	15	(7450)	
H_2O	15.74 (16.04)				(5.20 ± 0.37) × 10^{10}	

[a] pK_{AH} values from ref. 4.
[b] Statistically corrected values in parentheses.
[c] First-order rate constant
[d] Equation [16].
[e] Equation [12] + k_B[B].
[f] See text.

Table 6. Brønsted β values for general base catalysis of the cyclization of ethyl *p*-nitrophenylhydantoates.

Compound	β	No. of points	*r*
1-NPU	0.50 [a]	5	0.9559
2-NPU	0.58	5	0.9866
3-NPU	0.63	4	0.9638

[a] If the data for neutral phosphate are discarded, a slope of 0.60 is obtained in which case the point for alkaline phosphate falls on the correlation line.

Fig. 6. Brønsted plots of the rates GBC for the cyclization of **1**-NPU (△), **2**-NPU (●), and **3**-NPU (□). See text for linear relationships.

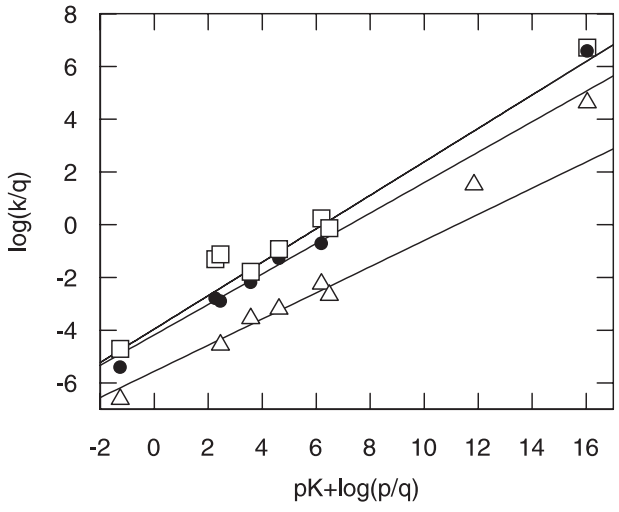

the rates for GBC showed the same saturation behaviour as observed with the OH^- catalysis. Figure 6 demonstrates how, except for the deviating points acid phosphate and glycine, the k_B values for **3**-NPU are insignificantly larger than those for **2**-NPU, though the increases for **2**-NPU over **1**-NPU amount to almost two orders of magnitude. This fact indicates that our previous conclusion (3) on the mechanism of GBC of the cyclization of ω-phenylhydantoic esters is incorrect. No data could be obtained for **1**-PUE. The similarity in the β values of ca. 0.6 for **2**-PUE and for **3**-PUE was interpreted as evidence of the same mechanism and the close catalytic constants as due to an early transition state with respect to ring formation, namely r.d. formation of T^- concerted with deprotonation of the ureido group. If the same mechanism applies to NPU, obviously it does not fit the large *gem*-dimethyl effect observed between **1**-NPU and **2**-NPU. The latter is compatible with two other possibilities. Either GBC of **3**-NPU involves a different mechanism than that of **1**- and **2**-NPU and the similar β values are accidental or all three involve GAC of the breakdown of T^-, the loss of

the *gem*-dimethyl effect with **3**-NPU being caused by steric hindrance to protonation. Actually the question can be answered within the framework of the mechanisms accepted for the rate profiles. GBC must comply with the rate-determining step of the reaction as a whole. Thus under conditions where formation of T^- is rate determining, the GBC reaction cannot proceed with r.d. breakdown unless the r.d.s. for the whole reaction is changed, a situation discussed above in relation to the curvature of the k_{obs} against fraction base plots. In the particular case of NPU, the r.d.s. in the various regions of the rate profiles are established above with a fair degree of certainty. The rate profiles (Fig. 1) indicate that the in whole region above pH 2.5 for esters **1**-NPU and **2**-NPU (the plateau and $k_{OH}{}^b$) where GBC was actually measured the reaction proceeds with rate-determining formation of T. Alternatively, under conditions where an equilibrium between reactant and T^- is established, as assumed for **3**-NPU above pH ca. 4, GBC formation of T^- cannot accelerate the reaction because the $[T^-]/[UH]$ ratio becomes time independent. Thus we have to conclude the **3**-NPU on the one hand and **1**-NPU–**2**-NPU on the other react by different mechanisms and that the similarity in β values is coincidental. Supporting evidence is the fact that the data for GBC by $H_2PO_4^{2-}$ and glycine with **3**-NPU deviate from the log k_B / p*K* correlation; in the low pH region a change in the r.d.s. is indicated by the rate profile.

Thus the best explanation for the loss of the *gem*-dimethyl effect in the GBC cyclizations of **3** appears once again to be a change to r.d. breakdown of the tetrahedral intermediate caused by steric hindrance to proton transfer as assumed by us for the OH^- catalysis of other ureido esters. Thus GBC with **1**-NPU and **2**-NPU has to be attributed to rate-determining formation of T^- concerted with deprotonation of the ureido group, structure **5**, while that with **3**-NPU to the general acid-catalyzed breakdown of T^-, structure **7**.[6]

Acknowledgments

We thank the National Foundation for Scientific Research of Bulgaria for funding this research and the Royal Society of Chemistry for a Journals Grant for International Authors (to I.G.P.).

References

1. I.B. Blagoeva, D.T. Tashev, and A.J. Kirby. J. Chem. Soc. Perkin Trans. 1, 1157 (1989).
2. C.K. Ingold. J. Chem. Soc. **119**, 305 (1921); C.K. Ingold, S. Sako, and J.F.Thorpe. J. Chem. Soc. 1117 (1922); N.L. Allinger and V. Zalkow. J. Org. Chem. **25**, 701 (1960); I.B. Blagoeva, B.J. Kurtev, and I.G. Pojarlieff. J. Chem. Soc. Perkin Trans. 2, 1115 (1979); A.J. Kirby. Adv. Phys. Org. Chem. **17**, 183 (1980); L. Mandolini. Adv. Phys. Org. Chem. **22**, 17 (1986).
3. E. Atay, I.B. Blagoeva, A.J. Kirby, and I.G. Pojarlieff. J. Chem. Soc. Perkin Trans. 2, 2289 (1998).
4. E. Atay, I.B. Blagoeva, and I.G. Pojarlieff. Dokl. Bolg. Akad. Nauk, **52**, No. 2, (1999). In press.
5. O. Belafdal, M. Bergon, M. Calmon, and J.P. Calmon. J. Org. Chem. **54**, 4193 (1989).
6. A.H. Koedjikov, I.B. Blagoeva, I.G. Pojarlieff, and A.J. Kirby. J. Chem. Soc. Perkin Trans. 2, 2479 (1996).
7. I.B. Blagoeva. J. Chem. Soc. Perkin Trans. 2, 127 (1987).
8. A.K. Covington, R.A. Robinson, and R.G. Bates. J. Phys. Chem. **70**, 3820 (1966); J.C. Fishbein and W.P. Jencks. J. Am. Chem.Soc. **110**, 5075 (1988).
9. D.F. Detar. J. Am. Chem. Soc. **104**, 7205 (1982).
10. F. Hibbert. Adv. Phys. Org. Chem. **22**, 113 (1986).
11. J. Kavalek, V. Sterba, and S. El Bahaie. Collect. Czech. Chem. Commun. **48**, 1753 (1983).
12. W.P. Jencks. Chem. Rev. **72**, 702 (1972).
13. W.P. Jencks. Acc. Chem. Res. **9**, 425 (1976).
14. K.J. Davies and M.I. Page. J. Chem. Soc. Chem. Commun. 1448 (1990).
15. T.C. Bruice. Annu. Rev. Biochem. **45**, 331 (1976).
16. R.A. More O'Ferrall. J. Chem. Soc. B: 274 (1970).
17. J. Kavalek, V. Machacek, G. Svobodova, and V. Sterba. Collect. Chech. Chem. Commun. **51**, 375 (1986).

[6] Tables of observed rate coefficients for 1-, 2-, and 3-NPU have been deposited as supplementary material (6 pages), which may be purchased from: The Depository of Unpublished Data, Document Delivery, CISTI, National Research Council Canada, Ottawa, Canada, K1A 0S2.